

Supplementary Information

Thin-film Conformal Fluorescent SU8-Phenylenediamine

Hani Barhum^{1,2,3,*}, Dennis Kolchanov^{2,3}, Mohammad Attrash⁴, Razan Unis^{1,5}, Janis Alnis⁶, Toms Salgals⁷, Ibrahim Yehia¹ and Pavel Ginzburg^{2,3}

¹Triangle Regional Research and Development Center, Kfar Qara' 3007500, Israel

²Department of Electrical Engineering, Tel Aviv University, Ramat Aviv, Tel Aviv 69978, Israel

³Light-Matter Interaction Centre, Tel Aviv University, Tel Aviv, 69978, Israel

⁴Andrew and Erna Viterbi Department of Electrical Engineering, Technion, Haifa

⁵*Department of Environmental Studies, Porter School of Environment and Earth Sciences, Tel Aviv University, Tel Aviv, Israel*

⁶Institute of Atomic Physics and Spectroscopy, University of Latvia, Jelgavas Street 3, 1004 Riga, Latvia

⁷Institute of Telecommunications, Riga Technical University, 12 Azenes Street, 1048 Riga, Latvia

Our exploration of fabrication conditions involved three phenylenediamine isomers: m-PD, o-PD, and p-PD. These isomers were made to react with SU8 2000.5 at a concentration of 1 mg/mL. Varying volumes of concentrated HCl were added to facilitate the conjugation reaction. With an increase in HCl volume, we observed a corresponding darkening in the color of the mixtures, hinting at a relationship between acid concentration and conjugation efficiency. This trend also extended to optical absorbance, with increased absorbance spectra below 500 nm corresponding to higher HCl volumes for all three isomers.

The properties of the conjugated materials distinctly varied for each phenylenediamine isomer. For o-PD and p-PD, the PLE spectra showed consistent trends in intensity with the addition of HCl, although fluorescence was notably lower in the absence of HCl. The emission spectra for both these isomers displayed an increase in intensity and a red

shift of the emission peak with higher HCl concentrations, reinforcing the notion that acid accelerates the conjugation process by catalyzing the opening of the epoxy ring and enhancing the reactivity of the amine group. Among the isomers, m-PD exhibited superior fluorescent characteristics, including defined excitation and emission peaks, and a higher emission intensity compared to the other isomers. The comprehensive spectra, analyses, and comparisons involving o-PD and p-PD are outlined in Figures S1 (a) to (f).

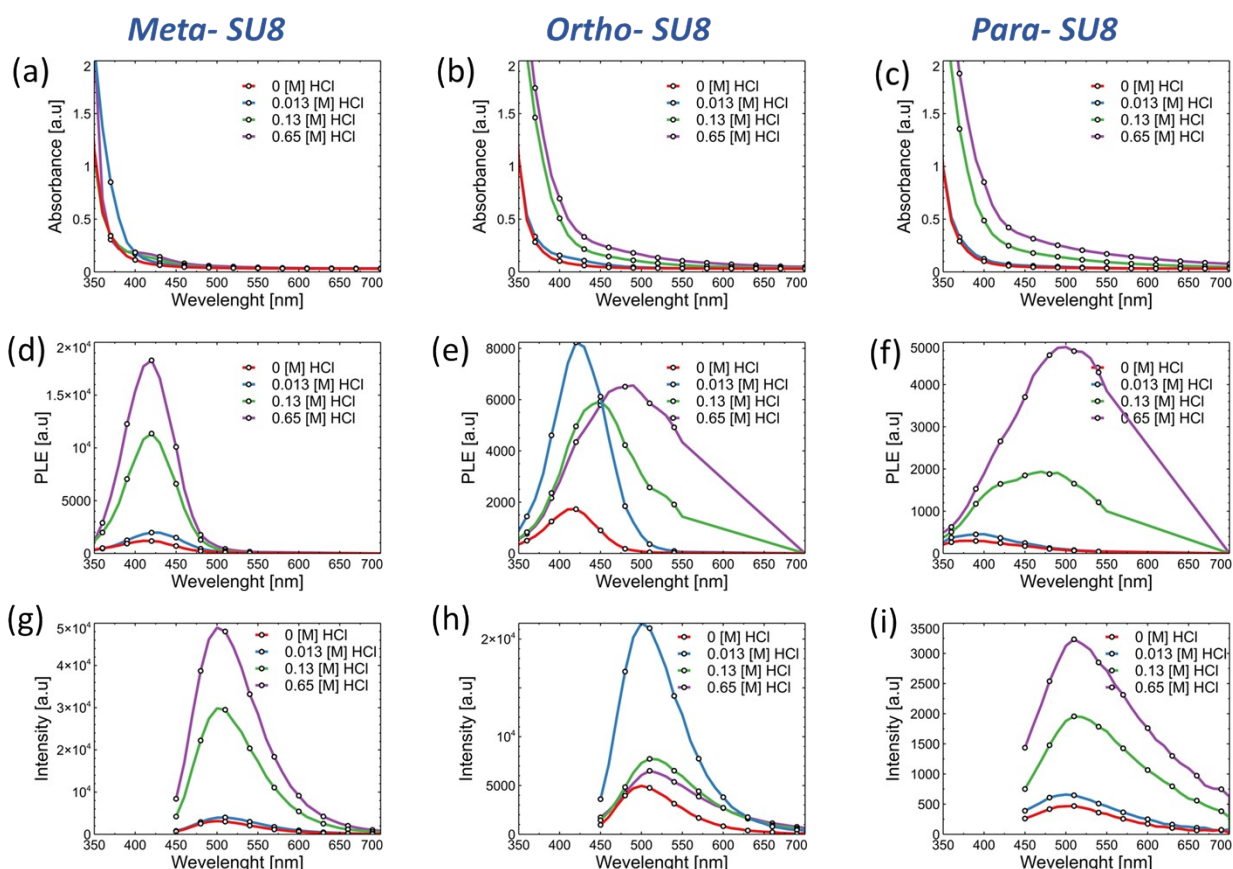


Figure S1. Comprehensive optical measurements of SU8 2000.5 conjugated with phenylenediamine isomers—meta, ortho, and para—arranged in columns, respectively. All data are presented in the wavelength range of 350 - 700 nm. The first row (a, b, c) displays the absorbance spectra at varying HCl concentrations, illustrating the impact of acid concentration on the conjugation reaction and the resulting optical properties. The second row (d, e, f) presents the photoluminescence excitation spectra, with emissions recorded at 580 nm, highlighting the excitation-dependent behavior of the conjugated

materials. Lastly, the third row (g, h, i) showcases the characteristic emission spectra obtained upon 420 nm excitation, offering insights into the unique photoluminescent. A meticulous examination of the emission responses of SU8-2000.5 to varied HCl concentrations and the detailed patterns of emission intensities for SU8-3005 and SU8-3050 are covered here. The enriched discussion is supported by Figures S2 providing extensive insight into the absorbance and emission behaviors across different SU8 polymers.

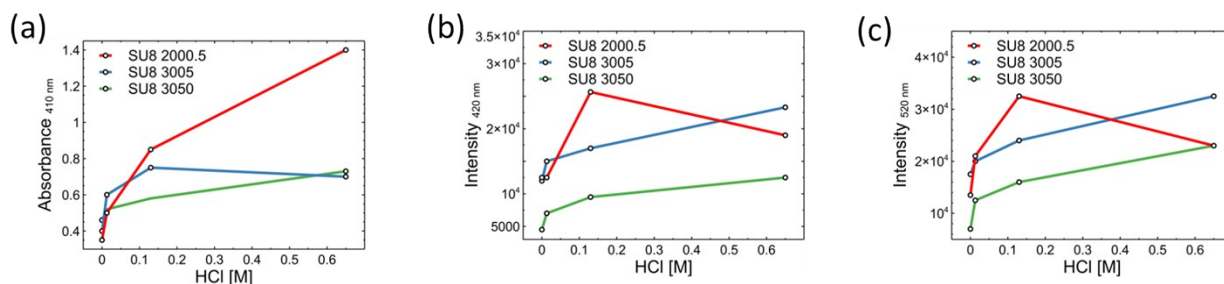


Figure S2. A comprehensive summary of the optical effects observed in absorbance, PLE, and emission spectra at various HCl concentrations for different SU8 polymers. SU8-2000.5 is represented in red, SU8-3005 in blue, and SU8-3050 in green. (a) Absorbance at 410 nm plotted against acid molarity, illustrating the influence of HCl concentration on the absorbance properties of the conjugated polymers. (b) PLE peak intensity - excitation at 420 nm with emission at 530 nm, showcasing the excitation-dependent behavior of the conjugated materials under varying acidity conditions. (c) Emission peak intensity at 520 nm, with 420 nm excitation, highlighting the impact of HCl concentration on the photoluminescent properties of the conjugated polymers.

XPS X-ray Photoelectron Spectroscopy (XPS)

Sample preparation for XPS involved spin coating the SU8-MPD solution onto carefully cleaned SiO₂ substrates. The analysis was conducted using a Canning 5600 AES/XPS multi-technique system (PHI, USA). This tool allows for detailed chemical analysis of solid materials, spanning from Li to U. It not only provides the atomic content but also sheds light on the chemical bonding of the surface atoms. For our specific case, the elemental analysis was accordingly derived.

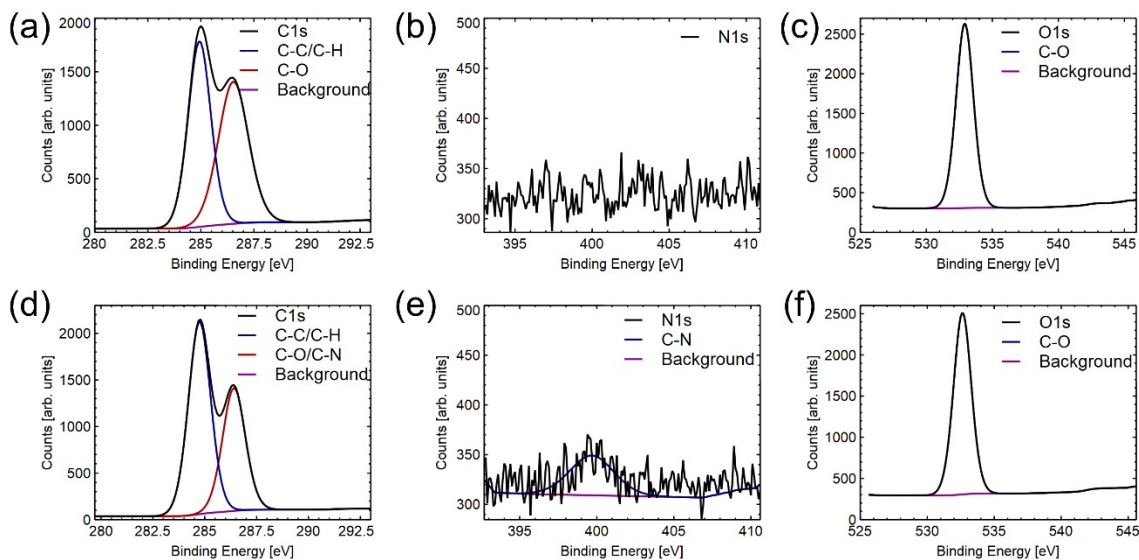


Figure S3: X-ray photoelectron spectroscopy (XPS) data illustrating the surface chemical composition and electronic state of SU8 and its conjugate with m-PD. (a) C1s spectrum of pure SU8. (b) N1s spectrum of pure SU8. (c) O1s spectrum of pure SU8. (d) C1s spectrum after m-PD conjugation. (e) N1s spectrum post m-PD integration. (f) O1s spectrum of the m-PD conjugated SU8.

SU8

Table S1. Peak data of XPS from SU8

Name	Peak BE	FWHM eV	Area (P) CPS.eV	Atomic %	Q
C 1s	285.35	4.23	353191.68	71.93	1
O 1s	532.67	3.91	275134.78	22.44	1
Si 2p	102.27	3.82	14116.43	2.93	1
F 1s	685.92	3.79	39294.96	2.50	1
S 2s	231.88	2.34	1338.03	0.20	1

SU8-mpd

Table S2. Peak data of XPS from SU8-mpd

Name	Peak BE	FWHM eV	Area (P) CPS.eV	Atomic %	Q
C 1s	285.34	4.19	351898.14	73.01	1
O 1s	532.64	3.87	263541.08	21.90	1
Si 2p	102.20	3.68	10354.82	2.19	1
F 1s	685.67	3.79	25941.20	1.68	1
N 1s	399.97	4.02	9296.99	1.22	1

Certainly! Here's a more compact and delicate representation:

- Determination of m-PD:SU8 Ratio Using XPS Data

Atoms in m-PD: - Carbon (C): 6 - Nitrogen (N): 2

Atoms in SU8 Monomer: - Carbon (C): 8 - Oxygen (O): 2

From this, we have:

$$[\%C_{\{m-PD\}} = 75\% \quad \%N_{\{m-PD\}} = 25\%]$$

$$[\%C_{\{SU8\}} = 80\% \quad \%O_{\{SU8\}} = 20\%]$$

Let (x) be the fraction of m-PD and ((1-x)) of SU8. Using XPS data for SU8-mPD:

$$[\%C = 73.01 \quad \%N = 1.22 \quad \%O = 21.90]$$

Using Carbon:

$$[75x + 80(1-x) = 73.01 \quad x_{\{C\}} = 0.0995]$$

Using Nitrogen:

$$[25x = 1.22 \quad x_{\{N\}} = 0.0488]$$

Using Oxygen:

$$[20(1 - x) = 21.90 \quad x_{\{O\}} = 0.055]$$

Given direct m-PD evidence from Nitrogen, our best minimum estimate is ($x_{\{N\}} = 4.88\%$). For the maximum, we use Carbon: ($x_{\{C\}} = 9.95\%$).

- Thus, the m-PD content in SU8-mPD is between 4.88% to 9.95%, leading to a m-PD:SU8 ratio between: **1:19.5** and **1:10.05**.

This is a concise representation that highlights the necessary calculations without extra verbosity.

DFT

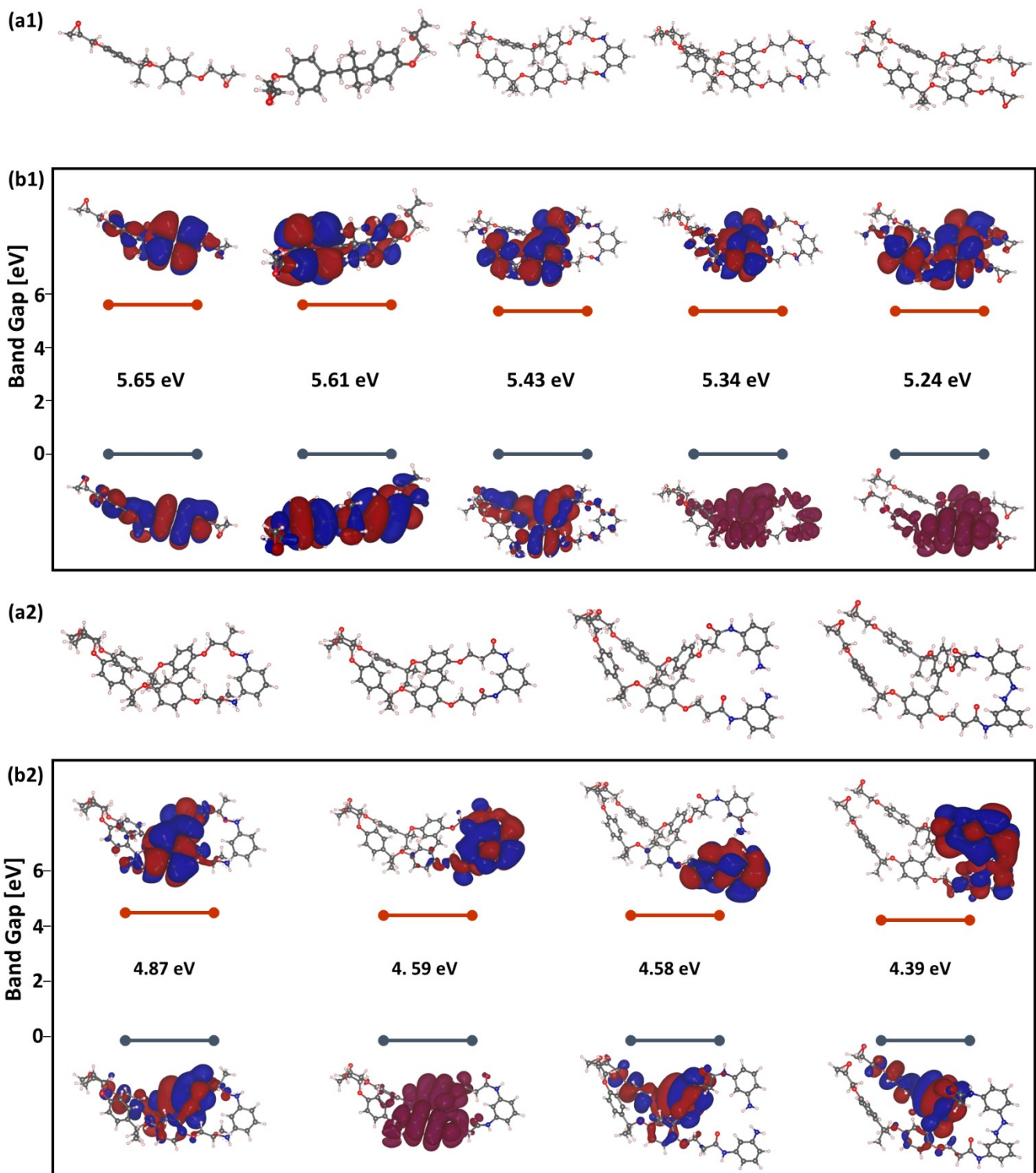


Figure S4: (a1, a2, b1, b2) Supplementary molecular structures demonstrating the potential conformations arising from the m-PD and SU8 interaction. The proposed

structures are arranged in decreasing band gap energies, suggesting their potential roles in generating the observed green emission. Additionally, the calculated band gaps of the respective structures, along with the corresponding HOMO and LUMO charge distributions, are presented for each conformation.

Supplementary Figure S4 provides a thorough exploration of potential molecular conformations that can arise from the interaction between m-PD and SU8 polymers, expanding beyond the structures highlighted in Figure 4.

In Supplementary Figure S4 (a1), the two leftmost structures represent the pristine SU8 monomers, setting the baseline for understanding the modifications induced by m-PD interaction. The subsequent two structures illustrate potential nitro (N-O) groups' formations. However, these configurations appear less likely, given their high calculated band gaps (ranging from 4.5 eV to 5.2 eV), which contrast with the green fluorescence observed experimentally.

In Figure S4 (a2) reiterates potential nitro (N-O) bond formations with slightly different configurations. As in the previous case, these structures' computed band gaps remain relatively high (around 3.6-4.5 eV), which doesn't coincide with the experimental observations of green fluorescence, indicating their less probable existence in the final composite. In Figure S4 (b1), we explore a scenario in which a single m-PD molecule interacts with one epoxy group from the SU8 polymer, leading to the formation of a secondary amine bond. This leaves the remaining epoxy group intact, potentially participating in further reactions. The band gap for this configuration falls within the range consistent with green emission, suggesting its plausible presence in the synthesized material. In Figure S3 (b2), the conformations further consider the possible formation of a secondary amine bond and subsequent hydroxyl group, as well as various N-C-C-O arrangements. While these structures present intriguing possibilities, the FTIR data does not provide direct evidence for these formations, marking them as less likely candidates.

The detailed exploration of potential molecular structures in the Supplementary offer a valuable insights into the complex molecular interplay underlying the m-PD-SU8 interaction. The main focus remains on the structures depicted in Figure 5, as their band gap values and FTIR evidence align more closely with the experimental data. However, the broad range of potential conformations underscores the dynamic and intricate nature of the polymer network, setting the groundwork for further studies into the relationship between molecular structure and optoelectronic properties in these materials.

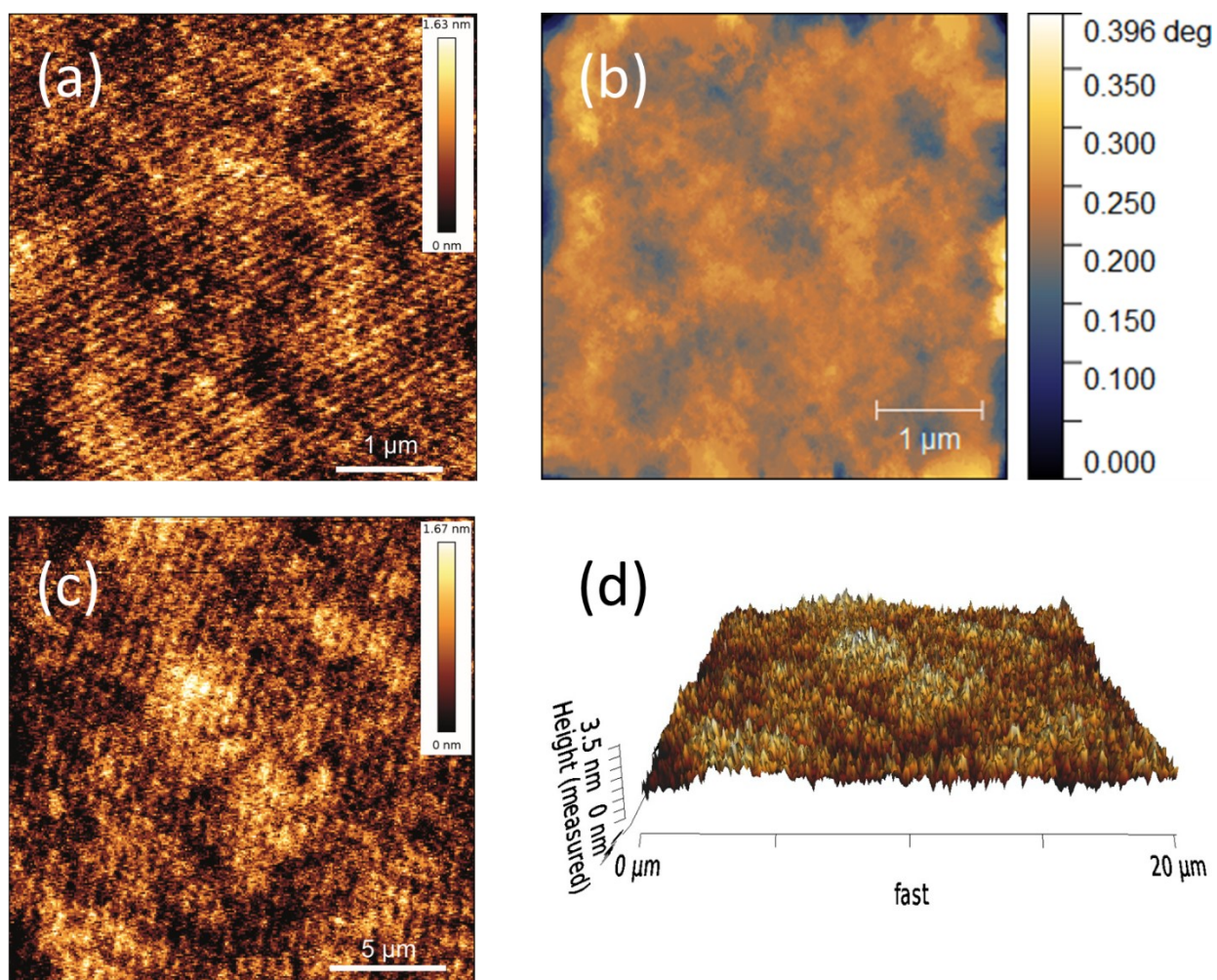


Figure S5. Atomic force microscopy (AFM) images of SU-8 conjugated with m-PD layers applied on glass. (a) High-resolution AFM topographic image of a small 5x5 μm area, including a 1 μm scale bar and height color map with scale. (b) Corresponding phase AFM image, revealing additional details of the surface structure. (c) Large-area

AFM image (20x20 μm) similar to (a), providing an overview of the sample surface. (d) 3D representation of the topography captured in (c), illustrating the complex surface features of the SU8-m-PD conjugate

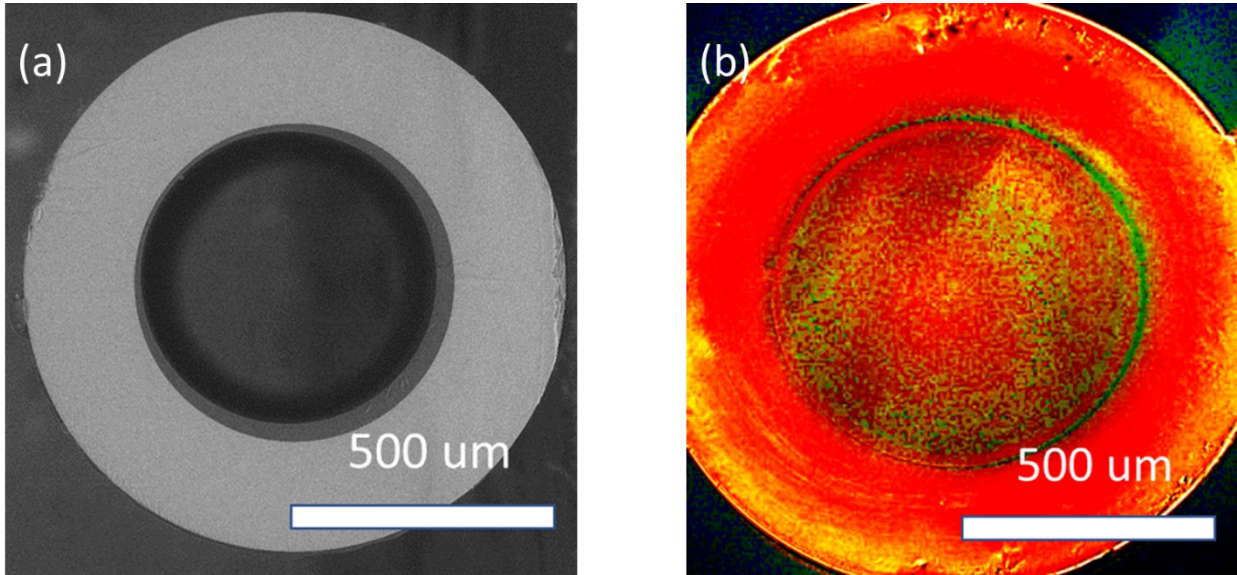


Figure S6. (a) Scanning Electron Microscopy (SEM) image of the capillary fiber, highlighting the surface morphology and structural composition of the SU8-m-PD composite. (b) Optical fluorescence image of the same capillary fiber, capturing the emission characteristics upon excitation.

DFT - CP2K input files

Geometry optimization input file

```
@SET PROJECT Project_name
```

```
@SET RUN GEO_OPT
```

```
@SET GUESS ATOMIC
```

```
&GLOBAL
```

```
PROJECT ${PROJECT}-geo-opt
```

```
RUN_TYPE ${RUN}
```

```
PRINT_LEVEL LOW
```

```
&END GLOBAL
```

```
&FORCE_EVAL
```

```
METHOD QUICKSTEP
```

```
STRESS_TENSOR ANALYTICAL
```

```
&PRINT
```

```
&STRESS_TENSOR
```

```
&END STRESS_TENSOR
```

```
&END PRINT
```

```
&DFT
```

```
LSD
```

```
BASIS_SET_FILE_NAME BASIS_MOLOPT
```

```
POTENTIAL_FILE_NAME POTENTIAL
```

```
&MGRID
```

```
NGRIDS 5
```

```
CUTOFF 300
```

```
REL_CUTOFF 60
```

```
&END MGRID
```

```
&QS
```

```
&END QS
```

```
&XC
```

```
&XC_FUNCTIONAL BLYP
&END XC_FUNCTIONAL
&END XC
```

```
&SCF
  MAX_ITER_LUMO 500
  EPS_SCF 1.0E-6
  SCF_GUESS ${GUESS}
  MAX_SCF 100
  &OUTER_SCF
    EPS_SCF 1.0E-5
    MAX_SCF 10
  &END
  &OT
  &END OT
&END SCF
```

```
&END DFT
```

```
&SUBSYS
  &KIND H
    ELEMENT H
    BASIS_SET TZVP-MOLOPT-GTH
    POTENTIAL GTH-BLYP
  &END KIND
  &KIND C
    ELEMENT C
    BASIS_SET TZVP-MOLOPT-GTH
    POTENTIAL GTH-BLYP
  &END KIND
  &KIND N
    ELEMENT N
    BASIS_SET TZVP-MOLOPT-GTH
    POTENTIAL GTH-BLYP
  &END KIND
  &KIND O
    ELEMENT O
    BASIS_SET TZVP-MOLOPT-GTH
    POTENTIAL GTH-BLYP
  &END KIND
  &CELL
    A 30.0 0.0 0.0
    B 0.0 30.0 0.0
    C 0.0 0.0 30.0
```

```
PERIODIC NONE
&END CELL
```

```
&TOPOLOGY
COORD_FILE_NAME ${PROJECT}.xyz
COORD_FILE_FORMAT XYZ
&END
```

```
&END SUBSYS
```

```
&END FORCE_EVAL
```

```
&MOTION
&GEO_OPT
TYPE MINIMIZATION
MAX_DR 1.0E-03
MAX_FORCE 1.0E-03
RMS_DR 1.0E-03
RMS_FORCE 1.0E-03
MAX_ITER 300
! OPTIMIZER CG
! &CG
! MAX_STEEP_STEPS 0
! RESTART_LIMIT 9.0E-1
! &END CG
&END GEO_OPT
```

```
&CONSTRAINT
&FIXED_ATOMS
COMPONENTS_TO_FIX XYZ
LIST 1
&END FIXED_ATOMS
&END CONSTRAINT
```

```
&END MOTION
```

Band gap calculation

```
@SET PROJECT Project_name
@SET RUN ENERGY
@SET GUESS RESTART
@SET FUNCTIONAL B3LYP
```

```
&GLOBAL
PROJECT ${PROJECT}-B3LYP
RUN_TYPE ${RUN}
PRINT_LEVEL LOW
&END GLOBAL

&FORCE_EVAL
METHOD QUICKSTEP

&DFT

LSD
BASIS_SET_FILE_NAME BASIS_MOLOPT
POTENTIAL_FILE_NAME POTENTIAL

&MGRID
NGRIDS 5
CUTOFF 300
REL_CUTOFF 60
&END MGRID

&QS
EPS_PGF_ORB 1E-20
EPS_FILTER_MATRIX 0.0E-20
&END QS

&AUXILIARY_DENSITY_MATRIX_METHOD
METHOD BASIS_PROJECTION
ADMM_PURIFICATION_METHOD MO_DIAG
&END

&POISSON
PERIODIC NONE
POISSON_SOLVER MT
&END POISSON

&XC
&XC_FUNCTIONAL ${FUNCTIONAL}
&END XC_FUNCTIONAL
&END XC

&SCF
MAX_ITER_LUMO 1000
```

```
EPS_SCF 1.0E-5
SCF_GUESS ${GUESS}
MAX_SCF 60
&OUTER_SCF
  EPS_SCF 1.0E-5
  MAX_SCF 10
&END
&OT
&END OT
&END SCF
```

```
&PRINT
  &PDOS
    NLUMO -1
    COMPONENTS
  &END
  &E_DENSITY_CUBE OFF
  &END E_DENSITY_CUBE
  &MO_CUBES
    NLUMO 1
    NHOMO 1
  &END
&END PRINT
```

```
&END DFT
```

```
&SUBSYS
&KIND H
  ELEMENT H
  BASIS_SET ORB TZVP-MOLOPT-GTH
  BASIS_SET AUX_FIT SZV-MOLOPT-GTH
  POTENTIAL GTH-BLYP
&END KIND
&KIND C
  ELEMENT C
  BASIS_SET TZVP-MOLOPT-GTH
  BASIS_SET AUX_FIT SZV-MOLOPT-GTH
  POTENTIAL GTH-BLYP
&END KIND
&KIND N
  ELEMENT N
  BASIS_SET TZVP-MOLOPT-GTH
  BASIS_SET AUX_FIT SZV-MOLOPT-GTH
  POTENTIAL GTH-BLYP
```

```
&END KIND
&KIND O
ELEMENT O
BASIS_SET TZVP-MOLOPT-GTH
BASIS_SET AUX_FIT SZV-MOLOPT-GTH
POTENTIAL GTH-BLYP
&END KIND
&CELL
  A 30.0  0.0  0.0
  B 0.0  30.0  0.0
  C 0.0  0.0  30.0
  PERIODIC NONE
&END CELL

&TOPOLOGY
  COORD_FILE_NAME ${PROJECT}-geo-opt.xyz
  COORD_FILE_FORMAT XYZ
&END

&END SUBSYS

&END FORCE_EVAL
```